Journal of Hazardous Materials 174 (2010) 437–443

Contents lists available at ScienceDirect

Journal of Hazardous Materials

journal homepage: www.elsevier.com/locate/jhazmat

Chemical and structural evaluation of activated carbon prepared from jute sticks for Brilliant Green dye removal from aqueous solution

Mohammad Asadullah[a,b,*], Mohammad Asaduzzaman[a], Mohammad Shajahan Kabir[a], Mohammad Golam Mostofa[a], Tomohisa Miyazawa[c]

[a] Department of Applied Chemistry and Chemical Technology, University of Rajshahi, Rajshahi, Bangladesh
[b] Curtin Centre for Advanced Energy Science and Engineering, Curtin University of Technology, 1 Turner Avenue, Technology Park, WA 6102, Australia
[c] Institute of Materials Science, University of Tsukuba, Tsukuba, Ibaraki 305-8573, Japan

ARTICLE INFO

Article history:
Received 26 June 2009
Received in revised form
13 September 2009
Accepted 14 September 2009
Available online 20 September 2009

Keywords:
Activated carbon
Chemical activation
Carbon structure
Surface chemistry
Adsorption

ABSTRACT

Activated carbons have been prepared from jute sticks by chemical activation using $ZnCl_2$ and physical activation using steam for the removal of Brilliant Green dye from aqueous solution. The activated carbons and charcoal prepared from jute sticks were characterized by evaluating the surface chemistry, structural features and surface morphology. The maximum BET surface area was obtained to be 2304 m^2/g for chemical activated carbon (ACC) while it is 730 and 80 m^2/g for steam activated carbon (ACS) and charcoal, respectively. The FT-IR spectra exhibited that the pyrolysis and steam activation of jute sticks resulted in the release of aliphatic and O-containing functional groups by thermal effect. However, the release of functional groups is the effect of chemical reaction in the $ZnCl_2$ activation process. A honeycomb-type carbon structure in ACC was formed as observed on SEM images. Although charcoal and ACC were prepared at 500 °C the ACC exhibited much lower Raman sensitivity due to the formation of condensed aromatic ring systems. Due to high surface area and high porous structure with abundance of functional groups, the ACC adsorbed dye molecules with much higher efficiency than those of ACS and charcoal.

1. Introduction

The effluents from textile, leather, paper, ink and cosmetic industries and also the industry that produces dyes are severely contaminated with dyes and pigments. Dyes in water even in very low concentration are visible and aesthetically are not acceptable. Since most of the dyes are toxic, the primary victim of dye toxicity is water biota. Long existence of dyes in water reservoir sometimes causes food chain contamination, resulting in deleterious health effect. Thus, the effluents containing dyes require proper treatment before being released into the environment. Different types of attempts have been made to separate dyes from industrial effluents among which adsorption [1–5], photocatalysis [6], biological treatment [7] and coagulation–flocculation [8] are a few of the examples. Although the biological treatment for the removal of organic compounds from water is effective to some extent the removal of organic refractory contaminants has been proven to be very ineffective. Therefore, the satisfactory results were obtained by adsorption method using different types of adsorbents [9].

Activated carbons, which can be produced from agricultural wastes, are known as very effective adsorbents for dye adsorption [10]. The unique properties of AC as adsorbents are due to their highly developed porosity, large surface area (usually 500–2000 m^2/g), skeletal structural features, variable characteristics of surface chemistry and high degree of surface reactivity [11].

Besides porosity, the chemical reactivity of AC surface significantly influences its adsorptive properties. The IR spectroscopic studies represented that during heat treatment at high temperature to produce AC, most of the reactive functional groups on the surface of biomass are released as H_2O, CO_2 and many other small molecules, leaving behind some less reactive oxide functional groups such as quinolic, etheric, phenolic and ketonic mostly on aromatic ring systems [12]. These surface oxides have acidic as well as basic properties depending on the ring structures [13]. The extent of ring condensation during activation has also a role to play to form a wide basal surface of AC, which facilitates the accommodation of dye molecules in adsorption. To elucidate the structural features of carbon materials, Raman spectroscopy has been used [14,15]. The study showed that during steam activation of char at 700–900 °C the structural features of carbon drastically changed due to the condensation of smaller ring systems (3–5 fused rings) to larger ring

* Corresponding author. Present address: Curtin Centre for Advanced Energy Science and Engineering, Curtin University of Technology, 1 Turner Avenue, Technology Park, WA 6102, Australia. Tel.: +61 8 9266 9655; fax: +61 8 9266 1138.
E-mail addresses: asad@ru.ac.bd, asadullah8666@yahoo.com, A.Mohammad@curtin.edu.au (M. Asadullah).

0304-3894/$ – see front matter © 2009 Elsevier B.V. All rights reserved.
doi:10.1016/j.jhazmat.2009.09.072

Table 1
Effect of temperature on the yield and specific surface area of activated carbons.

Carbon sample	Temperature (°C)	Activation burn-off (wt%)	Yield (wt%)	S_{BET} (m^2/g)
ACC	400	41.5	58.5	1968
	450	48.3	51.7	2104
	500	54.0	46.0	2304
	550	60.2	39.8	1872
	600	64.0	36.0	1744
ACS	500	81.3	18.7	450
	600	84.0	16.0	640
	700	88.0	12.0	730
	800	92.7	7.3	670
Charcoal	500	78.6	21.4	80

systems (≥6 fused rings) [16]. However, the studies on the structural features of chemically activated carbon are hard to find in the literature.

In this study activated carbons were prepared from jute stick using both physical and chemical activation methods. They were characterized by evaluating the surface chemistry with IR spectroscopy, structural features with Raman spectroscopy and surface morphology with scanning electron microscopy (SEM). The adsorption studies were carried out using Brilliant Green dye.

2. Experimental

2.1. Preparation of feedstock

Jute sticks were collected from local area, washed with distilled water, dried at 105 °C for 12 h and ground to 1–2 mm particle size. The physical properties, proximate and ultimate analyses of jute sticks have been published elsewhere [17]. The proximate analysis exhibited 76–78 wt% volatile fraction, 21–23 wt% fixed carbon and 0.62 wt% ash yield. The ultimate analysis resulted in 49.79 wt% C, 6.02 wt% H, 41.37 wt% O, 0.19 wt% N, 0.05 wt% Cl and 0.05 wt% S.

2.2. Preparation of activated carbon

2.2.1. Chemical activation method

About 10 g of dried jute sticks was mixed with $ZnCl_2$ solution and kept for about 12 h at room temperature. The $ZnCl_2$ to jute sticks ratio was adjusted to 1:1. The wet solid was then transferred into a stainless steel reactor, described elsewhere [18]. Before heating the reactor, nitrogen gas was purged for about 10 min at the rate of 200 mL/min to replace the air inside the reactor. Then the reactor was heated to 200 °C at the heating rate of 5 °C/min and was held at this temperature for at least 15 min. The temperature was further increased to activation temperatures ranging from 400 to 700 °C at the heating rate of 5 °C/min. The final product was repeatedly washed with hot deionised water until complete removal of $ZnCl_2$, confirming by the $AgNO_3$ test. Finally, the AC sample was dried at 105 °C for 24 h and stored in a desiccator. The activated carbon prepared by chemical activation method was denoted as ACC.

From the total weight loss due to the activation of jute sticks, the yields and activation burn-off were calculated, respectively using the following equations:

$$Y\,(\%) = \frac{M}{M_o} \times 100$$

$$Y'\,(\%) = \frac{M_o - M}{M_o} \times 100$$

where Y and Y' are yield of activated carbon and activation burn-off, respectively. M (g) is the mass of activated carbon obtained and M_o is the initial mass of jute sticks in dry basis.

2.2.2. Physical activation method

About 10 g of dry jute stick was placed into a stainless steel reactor, described elsewhere [19]. Briefly, the reactor was 20 cm long and 3 cm internal diameter with gas inlet and outlet system. Before heating the reactor, nitrogen gas was purged for about 10 min at the rate of 200 mL/min to replace the air inside the reactor. Then the reactor was heated to 700 °C at a heating rate of 5 °C/min under the nitrogen gas flow rate of 200 mL/min. When the temperature attained to 700 °C, the steam was started to flow at a rate of 75 mg/min through the char bed in the reactor. For steam generation, the water was supplied by a peristaltic pump into the upper hot zone of the reactor, where the water was suddenly vaporized and mixed up with nitrogen gas and went through the char bed. After completion of activation, the reactor was cooled. The activated carbons were collected and washed with 0.1 M HCl to remove ash and then washed with deionised water to remove residual acid. This activated carbon was denoted as ACS. A char was also prepared by pyrolyzing jute stick at 500 °C under nitrogen gas atmosphere.

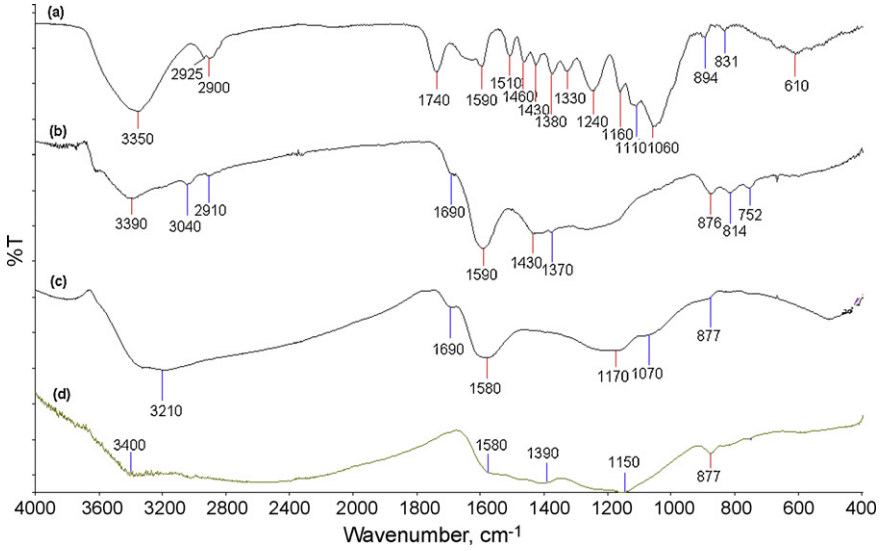

Fig. 1. FT-IR spectra of (a) jute sticks, (b) charcoal, (c) chemical activated carbon (ACC) and (d) steam activated carbon (ACS).

2.3. Characterization

2.3.1. Surface characterization

The BET surface areas of ACC, ACS and char were determined by nitrogen adsorption method at −196 °C using a Gemini Micrometrics (ASAP 2010). In order to know the surface functional groups, the FT-IR spectra of the samples were recorded between 4000 and 450 cm^{-1} using a PerkinElmer Spectrum GX FT-IR/Raman spectrometer. The structural features of activated carbons and char have been evaluated with the same PerkinElmer Spectrum GX FT-IR/Raman spectrometer equipped with an excitation laser of 1064 nm following the procedure developed elsewhere [14,15]. A back scattering configuration with an InGaAs detector was used to collect the spectra. The spectra in the range between 800 and 1800 cm^{-1} were curved-fitted with the GRAMS/32 AI software (version 6.0) using 10 Gaussian bands and a detailed discussion of Raman band assignments may be found elsewhere [14,15]. A scanning electron microscope (SEM) (Model JEOL 840) equipped with an energy dispersive X-ray microanalysis was used to determine the surface textural characteristics of the samples.

2.3.2. Dye adsorption

Brilliant Green dye was used for solution phase adsorption study of ACC. In each experiment 0.1 g ACC was added into 50 mL dye solution in a conical flask and shaken for a desired length of time in a thermostatic orbital shaker at 25 °C. After adsorption, the solution was filtered out and the concentration of the residual dye solution was measured using visible spectrophotometer (ANA–75) at λ_{max} 626 nm. The same experiment was also carried out for ACS and charcoal. The equilibrium adsorption of dye from different concentrations on ACC was measured to evaluate the Langmuir adsorption isotherm model. The amount of dye adsorbed, x/m was calculated and fitted to the following Langmuir equation:

$$\frac{C_e}{(x/m)} = \frac{1}{K_L \cdot x_m} + \frac{C_e}{x_m}$$

where C_e is the equilibrium concentration of solute remaining in the solution, x/m is the quantity of solute adsorbed per unit weight of adsorbent, and x_m and K_L are the Langmuir constants.

3. Results and discussion

3.1. Effect of temperature on the yield and surface area of activated carbons

The yields and specific surface areas of activated carbons prepared at different temperatures by chemical and physical activation are summarized in Table 1. In chemical activation process the activation burn-off occurred primarily by reacting activating agent with different functional groups of ligno-cellulosic materials, leading to dehydration, decarboxylation and condensation reactions. The reactions occurred in the chemical activation process were influenced by increasing activation temperature and thus progressively increased the activation burn-off, resulted in reduced yield of ACC. However, the BET surface area, which was created by the activation burn-off, increased only up to 500 °C. Further increase of temperature from 500 to 600 °C resulted in reduced surface area. This may be due to the loss of some pore walls due to excessive carbon burn-off.

In the physical activation and charcoal preparation processes the devolatilization of jute sticks occurred mainly at decomposition temperature [17]. During devolatilization, the aromatic ring systems of solid carbon significantly condensed to form polyaromatic ring systems. Therefore, the existence of pore became insignificant and thus the BET surface area of char was very low (80 m^2/g). Upon the addition of steam in physical activation process, the gasification of charcoal occurred, creating a number of pores. Consequently, the BET surface area significantly increased. The steam gasification reaction at lower temperature than 700 °C is less important [20]. Therefore, the surface areas at 500 and 600 °C are significantly low. The surface area attained to a maximum value (730 m^2/g) at 700 °C, which was further decreased with increasing temperature due to the destructive effect of over activation burn-off to the pore walls.

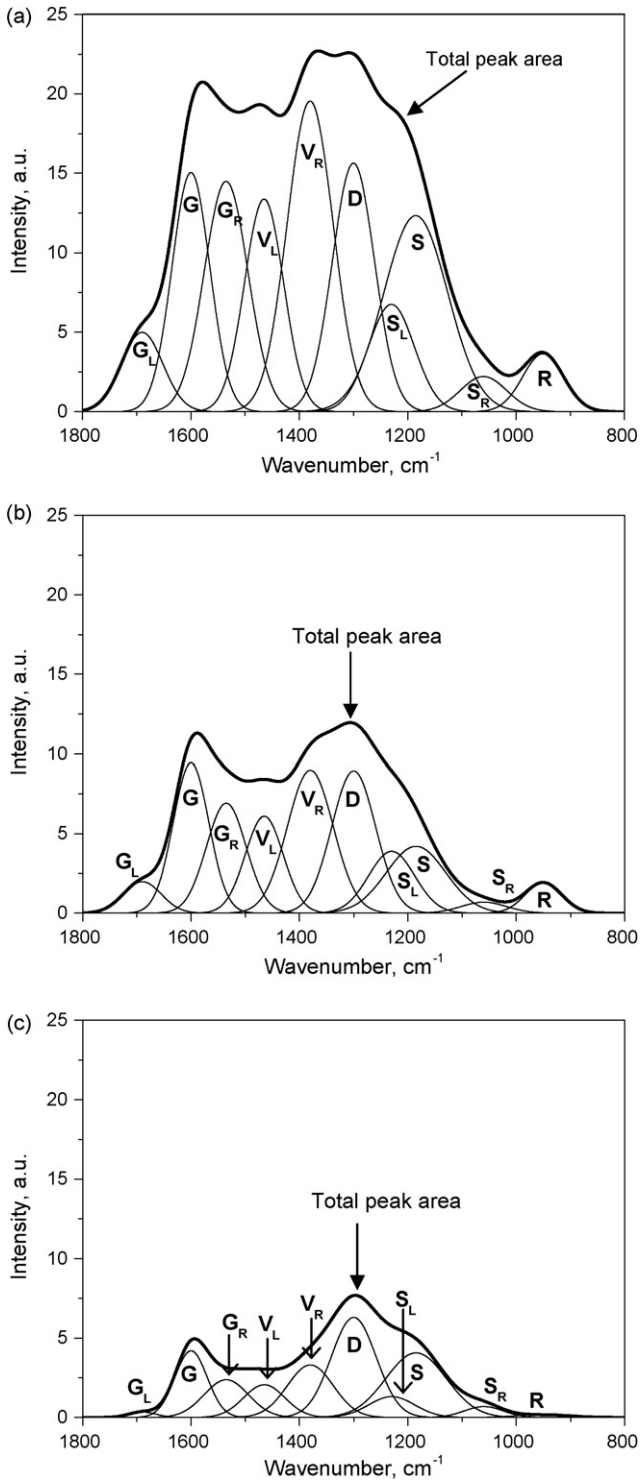

Fig. 2. Deconvolution of Raman spectra using 10 Gaussian bands for (a) charcoal, (b) ACC and (c) ACS. Charcoal and ACC were prepared at 500 °C and ACS was prepared at 700 °C.

Table 2
Peak areas of each of 10 Gaussian bands and total peak areas of three different samples.

Band name	Description	Peak intensity (a.u.)		
		ACS	ACC	Charcoal
G_L	Carbonyl group C=O	21.8	170.7	474.6
G	Graphite $E^2$2g; aromatic ring quadrant breathing; alkene C=C	312.7	786.5	1,302.9
G_R	Aromatics with 3–5 rings; amorphous carbon structures	242.9	611.5	1,499.0
V_L	Methylene or methyl; semicircle breathing of aromatic rings; amorphous carbon structures	196.0	561.0	1,212.0
V_R	Methyl group; semicircle breathing of aromatic rings; amorphous carbon structures	351.5	923.3	2,053.1
D	D band on highly ordered carbonaceous materials; C–C between aromatic rings and aromatics with not less than 6 rings	654.1	968.9	1,594.5
S_L	Aryl–alkyl ether; para-aromatics	139.8	370.9	652.7
S	$C_{aromatic}$–C_{alkyl}; aromatic (aliphatic) ethers; C–C on hydroaromatic rings; hexagonal diamond carbon sp^3; C–H on aromatic rings	567.4	588.2	1,851.3
S_R	C–H on aromatic rings; benzene (ortho-di-substituted) ring	62.0	80.6	236.7
R	C–C on alkanes and cyclic alkanes; C–H on aromatic rings	22.1	160.2	349.2
	Total peak area	2570.5	5221.7	11,226.1

3.2. Surface characterization

Dye adsorption on activated carbon from aqueous solution depends mainly on two typical properties such as surface area and surface functional groups. The increase of surface area more likely increases the number of accessible functional groups as well as the basal plane on the surface. The activated carbon has both polar sites due to the presence of oxygen containing functional groups and non-polar basal sites [21]. Since most of the dye molecules possess polar functional groups, they can preferentially be adsorbed on the polar sites of the activated carbon rather than the basal sites. It seems that the identification of surface chemical species is significant to promote the applicability of activated carbons for specific application. Although the identification of all the chemical species is not an easy task the information about the chemical nature of the carbon surfaces may be obtained using FT-IR spectroscopy.

Fig. 1 shows the FT-IR spectra of jute sticks charcoal, ACC and ACS over the wavelength range of 4000–400 cm^{-1}. The spectra exhibit that the functional groups on the jute stick surface significantly differ from those of charcoal, ACC and ACS. The following bands are observed on the spectrum of jute sticks (Fig. 1(a)). The broad band at 3350 cm^{-1} was ascribed to OH^- stretching vibration in hydroxyl groups of phenols. Two bands at 2925 and 2900 cm^{-1} were represented to asymmetric and symmetric stretching vibrations of the methylene group. Their bending vibrations were observed between 1430 and 1380 cm^{-1} [12,22]. The strong band at 1740 cm^{-1} was attributed to carbonyl group (C=O) [22]. The bands at 1590 and 1510 cm^{-1} were corresponded to the aromatic C=C bonds while a band at 1460 cm^{-1} was ascribed to aromatic methyl group ($-CH_3$) [23]. The C–O stretching or –OH deformation band in carboxylic acid was observed at 1430 cm^{-1} [12]. The bands at 1330 cm^{-1} could be attributed to C–O vibrations in carboxylate groups and the bands at 1240 and 1160 cm^{-1} could be attributed to esters (e.g. R–CO–O–R′), ethers (e.g. R–O–R′) or phenol groups. A shoulder at 1110 cm^{-1} and a relatively intense band at 1060 cm^{-1} could be assigned to alcohol (R–OH) groups. The C–H out of plane deformation and C–H out of plane bending in benzene derivatives caused the bands at 894 and 831 cm^{-1}, respectively.

As the spectra of charcoal in Fig. 1(b), some of the functional groups were completely disappeared while some were newly generated during pyrolysis of jute sticks. The bands at 3040 and 876 cm^{-1} are newly generated and corresponded to the =C–H and $=CH_2$ groups. The band at 814 and 752 cm^{-1} represented the C–H out of plane bending in benzene derivatives and C–H bending vibration in *cis*-RCH=CHR.

The FT-IR spectrum of chemical activated carbon (ACC) is exhibited in Fig. 1(c). The band at 3210 cm^{-1} was assigned to OH^- stretching vibration. Two significant aspects of this band were observed. Firstly, it had been shifted to the lower wave number and secondly, it was significantly broaden. These findings apparently suggested that the –OH group in the activated carbon was not free but more likely cross-linked. The band at 2900 cm^{-1} in raw jute sticks was completely disappeared from the ACC, leading to the significant decrease of aliphaticity in the activated carbon. Furthermore, the band at 1740 cm^{-1} in the spectrum of raw jute sticks was also disappeared, representing the complete removal of saturated aldehydes and ketones. The band at 1690 cm^{-1} was ascribed to stretching vibration of aryl ketone and the strong band at 1580 cm^{-1} attributed to the C=O stretching of carbonyl group in quinone structure [12]. The bands at 1170 and 1070 cm^{-1} are related to the condensed C–C–C bending. The spectrum of steam activated carbon (Fig. 1(d)) shows much lower intensity of the peaks. This is because the steam activation was carried out at 700 °C, much higher than that of the treatment temperature of charcoal and ACC. Consequently, most of the IR sensitive functional groups and aliphatic groups were removed.

3.3. Structural features

Fig. 2 shows the deconvoluted Raman spectra of charcoal, ACC and ACS. The areas of each of 10 Gaussian peaks as well as total peak areas for three different samples are listed in Table 2. As Fig. 2 and Table 2 show, the peak intensities decreased in the order of charcoal > ACC > ACS. The decrease in total Raman intensities reflected to the loss of O-containing functional groups and aliphatic groups and more significantly, the growth of condensed aromatic ring systems. These results supported the FT-IR results in Fig. 1. The total Raman intensity is affected by the Raman scattering ability and light absorptivity of the carbon materials [24]. As the temperature increased and steam reacted with carbonaceous materials for ACS, it became increasingly aromatic. The increasing aromaticity in ACS increased the light absorptivity [25] and thus decreased the Raman intensity. However, even though ACC was treated at the same temperature as charcoal (500 °C), the total Raman intensity and the intensity of each band decreased significantly. This was attributed to the elimination of O-containing functional groups and aliphatic groups by the chemical reaction of them with $ZnCl_2$.

The D band in the Raman spectra represented the highly condensed and ordered aromatic ring systems usually equal or more than 6 fused benzene rings. On the other hand, G_R, V_L, and V_R

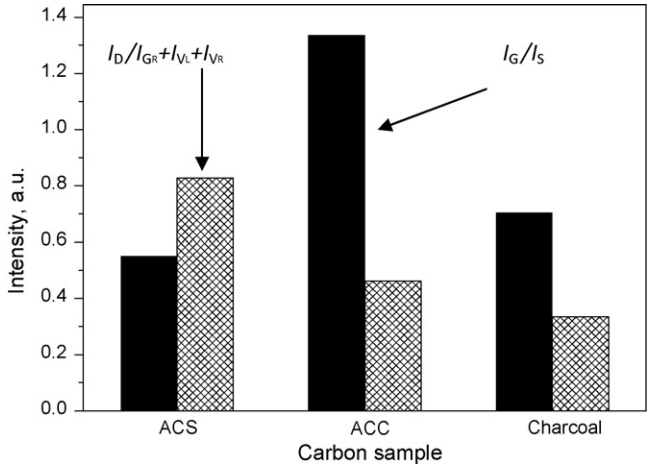

Fig. 3. The band intensity ratio $I_D/I_{(G_R+V_L+V_R)}$ and I_G/I_S of ACS, ACC and charcoal.

bands mainly corresponded to the 3–5 fused benzene rings with amorphous structure. Therefore, the ratio between the intensities of D band and the total intensities of bands G_R, V_L and V_R mainly attributed to the ratio of ordered carbons with larger ring systems to the amorphous and disordered carbons with smaller ring systems. The changes of the intensities of band area ratio between D and $G_R + V_L + V_R$ for charcoal, ACC and ACS are shown in Fig. 3. It can be seen that the ratio $I_D/I_{(G_R+V_L+V_R)}$ decreased in the order of ACS > ACC > charcoal. The results suggested that the increase of aromatic ring condensation in ACS was mainly due to the effect of higher temperature and in ACC is mainly due to the chemical reaction with $ZnCl_2$. Fig. 3 also exhibits the ratio I_G/I_S of different samples, which represents the intensity ratio between the band corresponds to the sp^2 carbon structure and the band corresponds to the sp^3 carbon structure. The ratio was significantly higher for ACC than other two. These results indicated that the wider sp^2 carbon structure possibly graphite structure of carbon in ACC contributed to the high basal surface area. In addition, the π electron of sp^2 carbon can readily be delocalized. Due to electron delocalizing nature of sp^2 carbon in ACC, the surface can be more efficient to adsorb polar dye molecules.

3.4. Textural characterization by scanning electron micrograph (SEM)

Fig. 4 shows the SEM images of (a) jute sticks, (b) charcoal, (c) ACS and (d) ACC. The images represent the morphological changes of the carbon materials during pyrolysis and activation. The jute stick surfaces are relatively smooth solid surface (Fig. 4(a)) with long ridges, resembling a series of parallel lines as observed in other biomasses [26]. When jute sticks were subjected to pyrolyze to produce charcoal, most of the organic volatiles were evolved, leaving behind the ruptured surface of charcoal with a small number of pores.

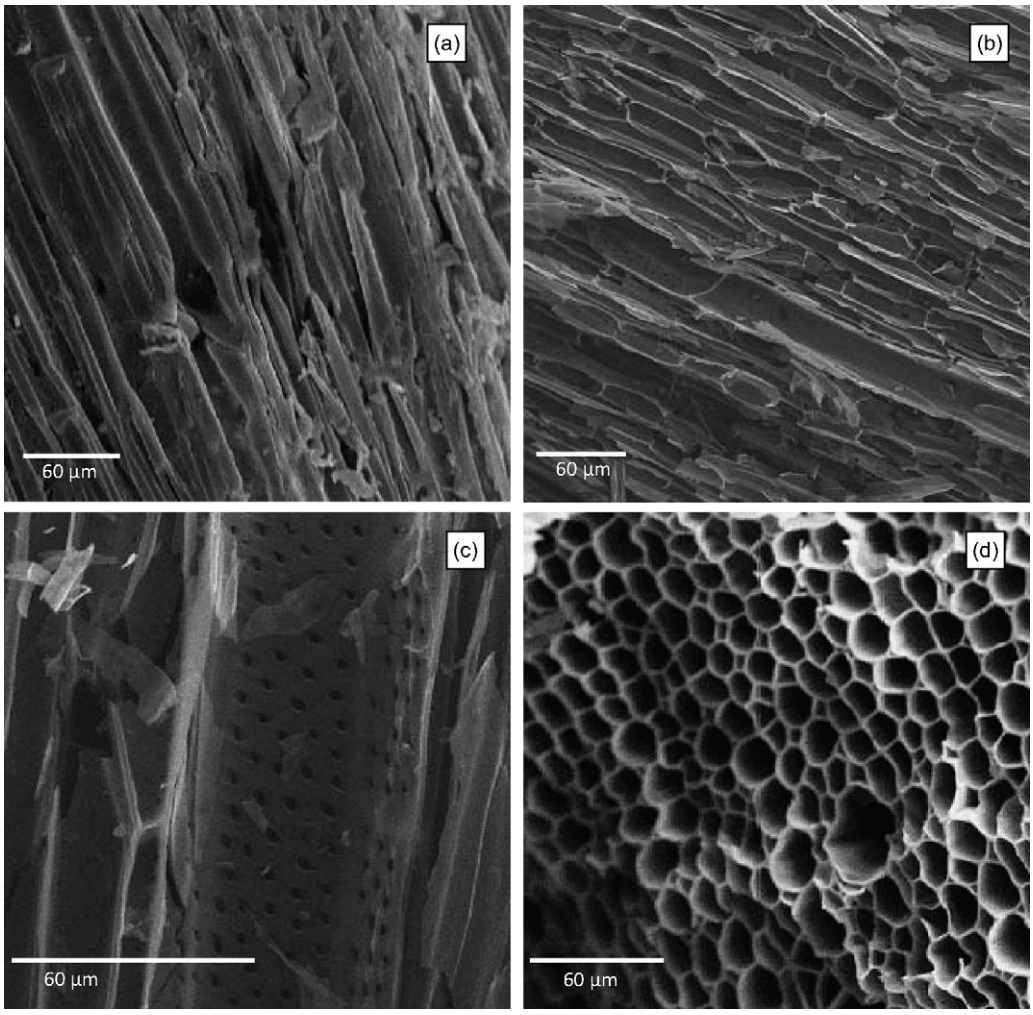

Fig. 4. Scanning electron micrograph of (a) jute sticks, (b) charcoal, (c) ACS and (d) ACC.

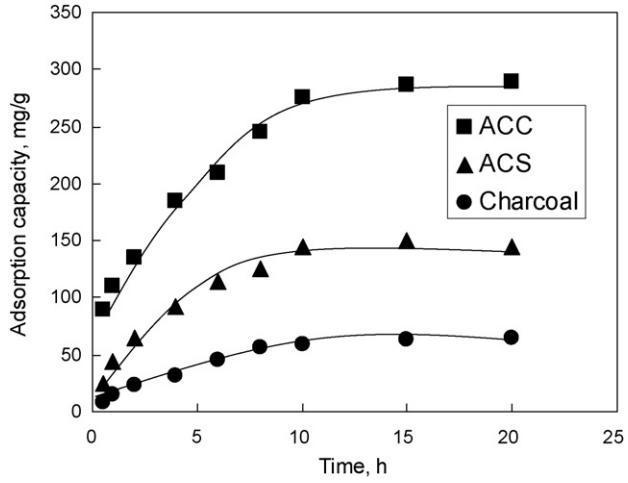

Fig. 5. Effect of contact time on Methylene Blue dye adsorption on ACC, ACS and charcoal at 25 °C.

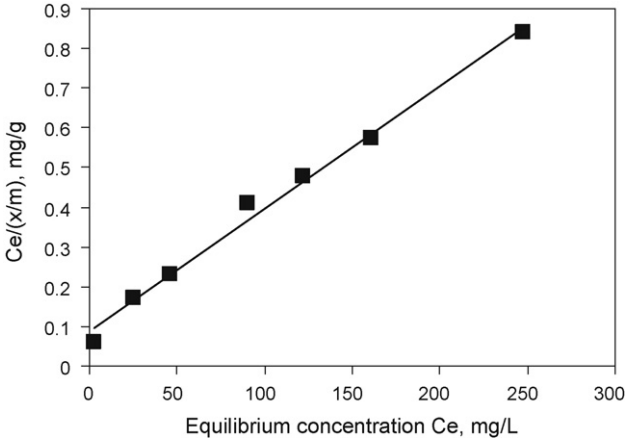

Fig. 6. Langmuir plot for the adsorption of methylene blue onto ACC at 25 °C.

The activation of charcoal with steam generated a number of different sizes of pores. This, thereby, increased the BET surface area from 80 m^2/g in charcoal to 750 m^2/g in ACS. From the comparison of the outer part of the charcoal and ACS with ACC, it is clear that the surface of jute sticks was deformed, resulted in well-developed pores with a honeycomb structure. This was possibly due to the extraction of some materials such as dissolution of lignin from jute sticks by activating agent during impregnation so as to create, on carbonization, a number of large macropores on the surface, generated a honeycomb structure. Although it is not clearly seen, a number of small pores were also generated on the walls of the honeycomb, contributed in the high surface area and adsorption properties.

3.5. Adsorption of Brilliant Green (BG) dye

Fig. 5 shows the BG adsorption capacity of three different adsorbents as a function of adsorption time. The concentration of dye solution (1000 mg/L) was higher than usual study [12] to determine the maximum adsorption capacity in a batch system at 25 °C. As in Fig. 5, charcoal has very limited BG adsorption capacity. The equilibrium adsorption obtained was 52 mg/g after 10 h. The equilibrium was attained within approximately 15 h for ACS with 150 mg/g adsorption capacity. However, the equilibrium adsorption was attained within 10–12 h for ACC with much higher adsorption capacity (286 mg/g) than other two.

The Langmuir adsorption isotherm was used to interpret the BG adsorption by ACC from the solution of different concentrations. Straight lines were fitted to the points in Fig. 6 by the method of least squares, where the slope of the regression line is $1/x_m$ and the intercept is $1/K_L \cdot x_m$. The linear regression lines obtained have highly significant correlation coefficients ($r^2 = 0.994$), indicating a good fit to the Langmuir equation. The essential feature of the Langmuir adsorption isotherm is a separation factor which is expressed by 'R_L', a dimensionless constant. It can be calculated by the following equation:

$$R_L = \frac{1}{1 + K_L C_0}$$

where C_0 is the highest initial dye concentration (mg/L) of the solution. The favourable value of R_L lies between 0 and 1. The experimental value of R_L obtained was 4.8×10^{-2}, leading to the favourable adsorption of BG onto the ACC [12].

4. Conclusion

A honeycomb-type highly porous activated carbon with high surface area (2304 m^2/g) has been prepared by the chemical activation of jute sticks using $ZnCl_2$. Steam activation of charcoal derived from jute sticks also resulted in porous activated carbon; however, the surface area was much lower than that of the chemical activated carbon. From the comparison of IR spectra, it is suggested that $ZnCl_2$ effectively removed the aliphatic and many of the oxygen containing functional groups from jute sticks, generating some new functional groups on the surface. For steam activated carbon, the elimination of functional groups is due to thermal effect. From the Raman spectra, it is revealed that the ACS is more condensed with more than six aromatic ring systems than ACC. However, from the ratio of I_G/I_S, it is suggested that the ACC is more graphitized than ACS, which is more favourable for the adsorption of dye from solution. It was reflected on Brilliant Green dye adsorption, which was much higher on ACC (480 mg/g) than that on ACS (182 mg/g). The Langmuir separation factor R_L was obtained to be 4.8×10^{-2} lies between 0 and 1, which is favourable value for efficient adsorption of dye.

Acknowledgement

This research was financially supported by the Third World Academy of Sciences (TWAS) under the project no.: 07-033 LDC/CHE/AS–UNESCO FR: 3240144818.

References

[1] Y.S. Al-Degs, M.I. El-Barghouthi, A.H. El-Sheikh, G.M. Walker, Effect of solution pH, ionic strength, and temperature on adsorption behavior of reactive dyes on activated carbon, Dyes Pigments 77 (2008) 16–23.
[2] Y.S. Al-Degs, M.A.M. Khraisheh, S.J. Allen, M.N. Ahmad, G.M. Walker, Competitive adsorption of reactive dyes from solution: equilibrium isotherm studies in single and multisolute systems, Chem. Eng. J. 128 (2–3) (2007) 163–167.
[3] G.M. Walker, L. Hansen, J–A. Hanna, S.J. Allen, Kinetics of a reactive dye adsorption onto dolomitic sorbents, Water Res. 37 (9) (2003) 2081–2089.
[4] G.M. Walker, L.R. Weatherley, Adsorption of dyes from aqueous solution—the effect of adsorbent pore size distribution and dye aggregation, Chem. Eng. J. 83 (3) (2001) 201–206.
[5] G.M. Walker, L.R. Weatherley, Kinetics of acid dye adsorption on GAC, Water Res. 38 (8) (1999) 1895–1899.
[6] A.O. Ibhadon, G.M. Greenway, Y. Yue, P. Falaras, D. Tsoukleris, The photocatalytic activity and kinetics of the degradation of an anionic azo-dye in a UV irradiated porous titania foam, Appl. Catal. B: Env. 84 (3–4) (2008) 351–355.
[7] N. Junnarkar, D.S. Murty, N.S. Bhatt, D. Madamwar, Decolorization of diazo dye Direct Red 81 by a novel bacterial consortium, World J. Microbiol. Biotechnol. 22 (2) (2006) 163–168.
[8] E. Guibal, J. Roussy, Coagulation and flocculation of dye-containing solutions using a biopolymer (Chitosan), React. Funct. Polym. 67 (1) (2007) 33–42.

[9] H. Lata, R.K. Gupta, V.K. Garg, Removal of basic dye from aqueous solution using chemically modified Parthenium Hysterophorus Linn biomass, Chem. Eng. Commun. 195 (10) (2008) 1185–1199.
[10] J.M. Dias, M.C.M. Alvim-Ferraz, M.F. Almeida, J. Rivera-Utrilla, M. Sanchez-Polo, Waste materials for activated carbon preparation and its use in aqueous-phase treatment: a review, J. Environ. Manage. 85 (2007) 833–846.
[11] R.C. Bansal, D. Aggarwal, M. Goyal, B.C. Kaistha, Influence of carbon–oxygen surface groups on the adsorption of phenol by activated carbons, Indian J. Chem. Technol. 9 (4) (2002) 290–296.
[12] A.L. Ahmad, M.M. Loh, J.A. Aziz, Preparation and characterization of activated carbon from oil palm wood and its evaluation on Methyl blue adsorption, Dyes Pigments 75 (2007) 263–272.
[13] H.P. Boehm, Surface oxides on carbon and their analysis: a critical assessment, Carbon 40 (2002) 145–149.
[14] X. Li, J–I. Hayashi, C–Z. Li, Volatilisation and catalytic effects of alkali and alkaline earth metallic species during the pyrolysis and gasification of Victorian brown coal. Part VII. Raman spectroscopic study on the changes in char structure during the catalytic gasification in air, Fuel 85 (2006) 1509–1517.
[15] D.M. Keown, X. Li, J–I. Hayashi, C–Z. Li, Characterization of the structural features of char from the pyrolysis of cane trash using Fourier Transform-Raman spectroscopy, Energy Fuel 21 (2007) 1816–1821.
[16] D.M. Keown, J–I. Hayashi, C–Z. Li, Drastic changes in biomass char structure and reactivity upon contact with steam, Fuel 87 (2008) 1127–1132.
[17] M. Asadullah, T. Miyazawa, S.-I. Ito, K. Kunimori, M. Yamada, K. Tomishige, Gasification of different biomasses in a dual-bed gasifier system combined with novel catalysts with high energy efficiency, Appl. Catal. A: Gen. 267 (1–2) (2004) 95–102.
[18] M. Asadullah, M.A. Rahman, M.A. Motin, M.B. Sultan, Preparation and adsorption studies of high specific surface area activated carbon obtained from chemical activation of jute stick, Adv. Sci. Technol. 24 (9) (2006) 761–770.
[19] M. Asadullah, M.A. Rahman, M.A. Motin, M.B. Sultan, Adsorption studies of activated carbon derived from steam activation of jute stick char, J. Surf. Sci. Technol. 23 (1–2) (2007) 1–8.
[20] M. Asadullah, S. Ito, K. Kunimori, M. Yamada, K. Tomishige, Biomass gasification to hydrogen and syngas at low temperature: novel catalytic system using fluidized-bed reactor, J. Catal. 208 (2) (2002) 255–259.
[21] L.R. Radovic, C. Moreno-Castilla, J. Rivera-Utrilla, Carbon materials as adsorbents in aqueous solutions, in: L.R. Radovic (Ed.), Chemistry and Physics of Carbon, vol. 27, Marcel Dekker, New York, 2000, pp. 227–405.
[22] T. Yang, A.C. Lua, Textural and chemical properties of zinc chloride activated carbons prepared from pistachio-nut shells, Mater. Chem. Phys. 100 (2–3) (2006) 438–444.
[23] P. Elham, S.M. Hamami, J. Zaihan, The carbonization of palm kernel shell by continuous kiln, in: Sixth Asia-Pacific International Symposium on Combustion and Energy Utilization, Universiti Teknologi Malaysia, Kuala Lumpur, Johor, May 20–22, 2002, 2002, pp. 308–312.
[24] X. Li, J.-I. Hayashi, C.-Z. Li, FT-Raman spectroscopic study of the evolution of char structure during the pyrolysis of a victorian brown coal, Fuel 85 (2006) 1700–1707.
[25] O. Ito, Diffuse reflectance spectra of coals in the UV-visible and near-IR regions, Energy Fuel 6 (1992) 662–665.
[26] B.G.P. Kumar, K. Shivakamy, L.R. Miranda, M. Velan, Preparation of steam activated carbon from rubber wood sawdust (*Hevea brasiliensis*) and its adsorption kinetics, J. Hazard. Mater. B 136 (2006) 922–929.